

# Rheological and tribological properties of seaweed powders as thickeners for liquid foods

Leyla Covacevich<sup>a,\*</sup>, José Miguel Aguilera<sup>a</sup>, M. Carolina Moreno<sup>a</sup>, Natalia Brossard<sup>b</sup>, Fernando Osorio<sup>c</sup>

<sup>a</sup> Department of Chemical and Bioprocess Engineering, Pontificia Universidad Católica de Chile, Macul 4860, Santiago, Chile

<sup>b</sup> Department of Fruticulture and Oenology, Faculty of Agronomy and Forestal Engineering, Pontificia Universidad Católica de Chile, Macul 4860, Santiago, Chile

<sup>c</sup> Department of Food Science and Technology, University of Santiago of Chile. Av. El Belloto 3735, Estacion Central, Santiago, Chile

## ARTICLE INFO

### Keywords:

Thickeners  
Seaweed  
Friction  
Rheological behavior  
Microstructure  
Saliva

## ABSTRACT

Thickened liquid foods are particularly interesting in culinary applications and the management of swallowing disorders. Polysaccharide molecules and suspended soft particles play a major role in increasing viscosity and mouthfeel. In this work, tribo-rheological effects of finely ground particles (less than 75  $\mu\text{m}$ ) of *Durvillaea antarctica* seaweed (SP) as a minimally processed and natural alternative to commercial thickeners were studied. Shear viscosity ( $\eta$ ), viscoelastic moduli ( $G'$ ,  $G''$ ), and the coefficient of friction (CoF) were determined for SP dispersions, using as controls two commercial thickeners: modified maize starch-based (TE) and xanthan gum-based (TU). SP and SP dispersions were characterized microstructurally and evaluated at concentrations of 1.2%, 2.4%, and 4.8% w/v, with and without artificial saliva (AS). SP dispersions exhibited a pseudoplastic behavior in the range of shear rates 0.1–100  $\text{s}^{-1}$  and viscoelasticity ( $G' > G''$ ) in the 0.1–80 rad/s frequency range. The incorporation of AS had a dilution effect in SP and TU dispersions, but additionally, in the case of TE, a hydrolyzing effect decreased the values of the responses. In the tribology experiments, all samples followed a Stribeck curve. SP dispersions were more lubricating than AS and controls in the physiological range of velocities during oral processing and swallowing (e.g., >100 mm/s). The thickening, viscoelastic, and lubrication behavior of SP dispersions were attributed to the soluble solids released from the SP (37%–51% d. w.) and interactions with ghosts of SP particles in the continuous aqueous phase. Fine seaweed particles may be a sustainable and low-cost alternative to commercial thickeners in some food applications.

## 1. Introduction

Sensorial perceptions of liquid foods are affected by dynamic physical phenomena occurring in the oral cavity, mediated by rheological (bulk) and tribological (surface) properties (Blok, Bolhuis, & Stieger, 2020; Krop, Hetherington, Holmes, Miquel, & Sarkar, 2019). For example, Kokini, Kadane, and Cussler (1977) suggested that the “thickness” of liquids was closely associated with viscous forces while “smoothness” was related to frictional forces. Oral processing of liquids has been largely associated with their rheological behavior (Rudge, Scholten, & Dijkman, 2019) but also to the lubrication by saliva between sliding surfaces, e.g., tongue-palate and tongue-oral mucosa (Pradal & Stokes, 2016; Shewan, Pradal, & Stokes, 2020). A recent study suggests that oral processing behavior is primarily driven by the rheological and lubrication properties of foods rather than by their taste

intensity (Gonzalez-Estanol, Libardi, Biasioli, & Stieger, 2022).

Polysaccharides and proteins are used as food thickeners to produce viscous liquids by modifying the internal structure of sauces, soups, dressings, and emulsions (Blok et al., 2021; Himashree, Sengar, & Sunil, 2022). Food biopolymers provide interesting lubricating and rheological properties to liquid foods (Hadde, Cichero, Zhao, Chen, & Chen, 2019; Kongjaroen, Methacanon, & Gamonpilas, 2022; Torres et al., 2019). Although refined thickeners (e.g., starch from plants and hydrocolloids from seaweeds) are expensive but quite convenient in liquid food formulation, the impact of processing on environmental sustainability and generation of waste is nowadays a matter of concern (Paraskevi et al., 2020).

Thickened liquid foods have been recommended for people with swallowing disorders, and several formulated thickeners are available on the market (Cichero, 2018; Laguna, Hetherington, Chen, Artigas, &

\* Corresponding author.

E-mail address: [lcovacevich@uc.cl](mailto:lcovacevich@uc.cl) (L. Covacevich).

<https://doi.org/10.1016/j.foodhyd.2024.110116>

Received 16 February 2024; Received in revised form 7 April 2024; Accepted 16 April 2024

Available online 21 April 2024

0268-005X/© 2024 Elsevier Ltd. All rights reserved.

Sarkar, 2016). Commercial thickeners for people with swallowing disorders are expensive and difficult to acquire for part of the population, thus, cheaper alternatives are needed (Schmidt, Komerowski, Steemburgo, & Oliveira, 2021).

Gum-based and starch-based thickeners are used to provide lubrication during oral processing and increase the viscosity of bolus, thus decreasing its velocity during swallowing (Ben Tobin et al., 2020; Cichero et al., 2017; Vieira et al., 2020). The incorporation of saliva in the oral cavity contributes to structural changes in the bolus formation (Devezeaux de Lavergne, Van de Velde, & Stieger, 2017; Torres et al., 2019). Secreted saliva hydrates particles to produce a paste-like bolus, susceptible to enzymatic breakdown from amylase and subsequent changes in bolus rheology (Stokes, Boehm, & Baier, 2013). Rheology and tribology properties are altered in starch-based thickeners due to interactions with amylase, leading to a decrease in viscosity and boundary lubrication and an increase in the coefficient of friction (Baixauli, Dobiasová, Tarrega, & Laguna, 2023; Torres et al., 2019). Furthermore, starch-based thickeners increase the residence time of bolus in the pharynx, leaving post-deglutition residues that can be easily aspirated (Hadde et al., 2019). Gum-based thickeners are recommended due to their stability, less likelihood of reacting with chemical components in saliva, and the tendency to form a stable entangled structure that improves the cohesiveness of the bolus (Aguilera & Covacevich, 2023; Kongjaroen et al., 2022; Torres et al., 2019). Additionally, from a tribological point of view, polysaccharides facilitate interactions with mucins and adhere to the oral surface (You & Sarkar, 2021).

Tribological properties have been correlated with mouthfeel sensations such as creaminess, astringency, and smoothness, a domain that rheological behavior does not sufficiently describe (Blok et al., 2020; Kokini et al., 1977; Krop et al., 2019; Sarkar, Andablo-Reyes, Bryant, Dowson, & Neville, 2019). Tribology is commonly used to study the lubricating properties of biopolymer-based thickeners during oral processing and swallowing (Blok et al., 2021; Sarkar et al., 2019; Vieira et al., 2020). However, less work has been done on the effect of particle dispersions as food thickeners. Minute soft particles dispersed in polymer solutions are known to alter the rheological and tribological properties of food suspensions (Chojnicka-Paszun, Doussinault, & De Jongh, 2014; Shewan, Pradal, & Stokes, 2020; Windhab, 1995).

Seaweeds are actively investigated as an abundant, low-cost, and sustainable source of novel food ingredients, natural bioactive compounds, and fiber (Figueroa, Farfán, & Aguilera, 2021; Peñalver et al., 2020). *Durvillaea antarctica* (commonly known in Spanish as *cochayuyo*) is a long cylindrical brown seaweed found abundantly on the coasts of Chile and southern New Zealand and consumed after cooking or utilized to extract alginates. Morphologically, the seaweed shows three important structures in cross-section: an outer cortical zone formed by a radial row of large cells, the intermediate medullary zone of interwoven hyphae, and a large hollow core formed by air-filled cavities separated by thin septa (Mateluna, Figueroa, Ortiz, & Aguilera, 2020). Seaweeds such as *D. antarctica* and several other brown seaweeds have a large proportion of fiber (e.g., cellulose) and up to 40% alginate on a dry-weight (d.w.) basis (Flórez-Fernández, Domínguez, & Torres, 2019; Gao et al., 2018; Rioux, Beaulieu, & Turgeon, 2017). However, producing highly purified, food-grade hydrocolloids from seaweed results in low yields and the utilization of chemicals and solvents that generate large amounts of waste (Jönsson, Allahgholi, Sardari, Hreggviðsson, & Nordberg Karlsson, 2020). Thus, current efforts aim at using semi-refined ingredients from seaweeds as well as waste algae to replace purified food thickeners. Malafronte et al. (2021) found that brown macroalgae treated mechanically and thermally enhanced the viscosity and viscoelastic properties of aqueous suspensions. Gao et al. (2018) demonstrated that cellulose nanofibers derived from waste brown seaweed when suspended in water, exhibited high viscosity, shear-thinning behavior, and good thickening properties.

To our knowledge, unprocessed seaweed particles have not been explored as natural thickeners for liquid foods. We hypothesize that fine

*Durvillaea antarctica* particles dispersed in water would release polymers (i.e., hydrocolloids) from broken cells that, together with the cellular remnants, will promote high viscosity and lubrication effects in liquids. In addition, seaweed may provide fiber, nutrients, and bioactive components at a lower cost and generate less waste than commercial thickeners. Thus, the objectives of this study are to prove the hypothesis by physically characterizing the particles and conducting rheological and tribological experiments.

## 2. Materials and methods

### 2.1. Raw materials and reagents

*Durvillaea antarctica* seaweed (*cochayuyo*) was harvested and sundried in December 2021 near Puerto Montt, Chile (41°27'56.66"S; 72°56'34.4"W). Dried algae were stored in plastic bags at room temperature until their use. *D. antarctica* contains 10.4% protein, 0.8% lipids, and 71.4% dietary fiber, including 35%–50% alginate (Kelly & Brown, 2000; Ortiz et al., 2006). The dry seaweed (moisture content of 10%) was ground into powder (SP) using a Thermomix food processor (Vorwerk, Wuppertal, Germany) at 5800 rpm for 1 min, followed by stone grinding with a Spectra 11 stone Melanger (Spectra, USA) for 4 h at 75 rpm. The powder was sifted to obtain a particle size fraction of less than 75 µm in an N°200 Tyler screen (Haver & Boecker Tyler, Ohio, USA).

Two commercial thickeners used for the treatment of swallowing disorders were the controls (Bolivar-Prados, Tomsen, Arenas, Ibáñez, & Clave, 2021): Thicken Up Clear (TU), a xanthan gum-based and maltodextrin thickener (Nestlé S.A, Vevey, Switzerland), and Thick & Easy (TE) modified maize starch based (Hormel Food Corp., MN). Reagents for artificial saliva (see below) were purchased from Sigma-Aldrich (Burlington, MA). Urea was obtained from Fermelo S.A. (Santiago, Chile). Distilled water was used to prepare the aqueous suspensions and the artificial saliva.

### 2.2. Preparation of samples and artificial saliva

The term “dispersions” is used to refer jointly to the aqueous suspensions of SP and the solutions of commercial thickeners. Aqueous dispersions of SP and the thickeners (TE and TU) were prepared at 1.2%, 2.4%, and 4.8% w/v concentrations to meet instructions for commercial thickeners and achieve low to high consistencies. Samples were prepared by dispersing the powders in distilled water using a hand blender (Braun, Germany) for 2 min at 3000 rpm. All dispersions were left to hydrate for 20 min before use.

Artificial saliva (AS) was prepared based on previous methods (Krop et al., 2019; Minekus et al., 2014). Briefly, artificial saliva was composed of 1.6 g/L NaCl, 0.33 g/L NH<sub>4</sub>NO<sub>3</sub>, 0.64 g/L K<sub>2</sub>HPO<sub>4</sub>, 0.2 g/L KCl, 0.31 g/L K<sub>3</sub>C<sub>6</sub>H<sub>5</sub>O<sub>7</sub>·H<sub>2</sub>O, 0.02 g/L C<sub>5</sub>H<sub>3</sub>N<sub>4</sub>O<sub>3</sub>Na, 0.2 g/L NH<sub>2</sub>CONH<sub>2</sub>, 3 g/L porcine mucin-type II (to adjust the viscosity of saliva), 0.15 g/L C<sub>3</sub>H<sub>5</sub>O<sub>3</sub>Na and 0.5 mL α-amylase of 1500 U/mL. AS contained 99.35% of water. To simulate oral conditions, a blend of dispersions containing artificial saliva was prepared according to the protocol by Ben Tobin et al. (2020) & Krop et al. (2019). The dispersions and artificial saliva were adjusted in a 1:0.5 v/v ratio.

In summary, the following nomenclature is used to refer to samples: *D. antarctica* seaweed powder (SP); TU (Thicken up clear, xanthan gum-based); TE (Thick & Easy, modified maize starch-based). Suspensions having added artificial saliva are followed by AS.

### 2.3. Soluble solids of SP dispersions

Soluble solids released from SP dispersions were determined by centrifuging 15 g of dispersions at different concentrations in a Heraeus Megafuge 8 R centrifuge (Thermo Scientific, Gotinga, Germany) at 10,000×g for 60 min and 37 °C. For each treatment, three samples of the

liquid phase (supernatant) and the pellet (sediment) were dehydrated in a DHG-9076 A forced air convective drying oven (Shanghai Longyue Instrument Equipment Co., China) for 180 min at 105 °C until constant weight. The weights of both supernatant and sediment were recorded before and after dehydration.

## 2.4. Characterization of particles and morphological aspects

### 2.4.1. Particle size distribution (PSD)

PSD of the seaweed powder and particles in seaweed dispersions with and without artificial saliva was determined by laser light scattering in a Malvern Mastersizer 2000 connected to a Hydro2000MU dispersion unit (Malvern Instruments Ltd, Worcestershire, UK). Samples were dispersed in water at room temperature under a stirring speed of 3000 rpm, followed by sonication at 10% amplitude for 5 s. A refractive index of 1.53 for particles and 1.33 for the aqueous dispersant was used, and the absorption index was set to 0.1. The particle size distribution was calculated using the instrument software from the intensity profile of the scattered light. The size distribution percentile  $d_{0,9}$ , volume-weighted mean diameter ( $D_{4,3}$ ), and uniformity of particles were obtained. The average and standard deviation of three measurements were reported.

### 2.4.2. Light microscopy

Optical microscopy was performed using an Olympus BX61 TRF bright field microscope (Olympus Corporation, Tokyo, Japan) equipped with an Omax 18 MP USB 3.0 C microscope digital camera (Omax microscope, China). Samples of the seaweed powder and seaweed dispersions were placed onto glass slides, covered with a coverslip, and observed under 20 × magnification. At least eight images were captured for each sample. OMAX software was used to collect the images, and Image J 1.54 d software (National Institute of Health, USA) was used for image processing and analyses. Image processing consisted of calibrating the image to 8-bit, subtracting the background, disabling smoothing, and modifying the light background between 500 and 600 pixels. The image was cropped, and the scale bar was inserted.

### 2.4.3. Field emission scanning electron microscopy (FESEM)

The seaweed powder and the SP dispersion at a concentration of 4.8% w/v with and without artificial saliva were studied by FESEM. The dispersion was poured into a Petri dish, frozen in liquid nitrogen, and freeze-dried for 72 h in a vacuum freeze-dryer model 4.5 L (Labconco Corporation, Kansas City, KS). Powders and freeze-dried samples were fixed onto a specimen holder with a carbon conductive adhesive tape and coated with gold (10 nm thickness) using a 108 Auto/SE Sputter Coater (Ted Pella, Inc., USA). The observation was performed in a Quanta™ FEG 250 (FEI Technologies Inc., OR, USA) at an accelerating voltage of 10kV.

## 2.5. Rheological measurements

Shear viscosity determinations and oscillatory frequency sweeps were performed in a rheometer Discovery DHR-2 (TA Instruments Ltd., New Castle, USA) using a plate-and-cone geometry with a diameter of 60 mm, gap of 27 μm and at a temperature of 37 °C to mimic conditions in the oral cavity. Thickeners and SP dispersions with and without artificial saliva were held in the rheometer for 5 min before starting the measurements to ensure that they had equilibrated to the set temperature. A water seal was used to prevent dehydration of the sample. The shear viscosity was measured during a steady state flow sweep in the shear rate range from 0.1 to 100 s<sup>-1</sup> and then reversed from 100 to 0.1 s<sup>-1</sup>. The elastic modulus  $G'$  and the viscous modulus  $G''$  were determined by oscillatory sweep tests in the frequency range of 0.1–80 rad/s and reversed. A strain amplitude sweep test was performed to find the strain amplitude in the linear viscoelastic region. The strain range of 0.1–10% was chosen. A strain amplitude was 0.5% in SP and TE

dispersions and 6% in TU dispersions. The strain amplitude of dispersions was used for the frequency sweep tests. Before the test, the samples were allowed to stand for 20 min for appropriate hydration. The measurements were done in duplicate.

To investigate the time-dependent thinning flow curves without and with artificial saliva, the relative thixotropic area (RTA) was calculated by integrating the area upstream and downstream curves and the hysteresis loop divided by the area under the upstream shear curve. This parameter has been suggested as suitable when comparing products with different viscosities (Badia-Olmos et al., 2022).

## 2.6. Tribology measurements

Tribological measurements of the samples at different concentrations were conducted in a Mini Traction Machine (MTM2, PCS Instruments Ltd., London, UK) using a ball-on-disk configuration to facilitate a mixed rolling and sliding contact. A 19 mm diameter ball (representing the palate) and a 46 mm diameter disc of a thickness of 4 mm, both made of polydimethylsiloxane (PDMS) and having a surface average roughness of  $R_a < 50$  nm, were used. Thickeners and SP dispersions without and with artificial saliva were loaded into the pot on the disc using a pot-filler, and the ball was lowered onto the disc. The slide-to-roll speed ratio was set to 50% and represents the relative surface velocities of the ball and disc; the rolling speed was varied from 1 mm/s to 1000 mm/s in order to obtain the boundary, mixed, and hydrodynamic regimes of the Stribeck curve. An applied load of 1 N and a temperature of 37 °C were selected, simulating oral conditions (Krop et al., 2019; Torres et al., 2019). Before each experiment, the tribopairs were cleaned with 2% sodium dodecyl sulfate solution and rinsed with distilled water. The coefficient of friction (CoF) was calculated as the friction force divided by the applied load ( $CoF = F_f/W$ ). An average of two measurements were reported.

## 2.7. Statistical analysis

Data were subjected to analysis of variance (ANOVA), and the means were compared using Tukey's test to determine whether statistically significant differences existed between the samples ( $p < 0.05$ ). The effect of the sample formulation on rheological and tribological behavior as a function of concentration was analyzed by one-way ANOVA. Statistical analysis was carried out using OriginPro 2015 software (OriginLab Corporation, Northampton, MA).

## 3. Results and discussion

### 3.1. Effect of particle size distribution on seaweed powder particles

PSD of the SP and SP aqueous dispersions (1.2%, 2.4%, 4.8% w/v) with and without artificial saliva (AS) are shown in Fig. 1. SP particles and SP particles in aqueous dispersions showed a polydisperse and homogeneous monomodal distribution with similar width of the PSD curves. PSD curves showed that 90% of the particles from all samples had a size ( $d_{0,9}$ ) smaller than ca. 150 μm (Table 1). This suggests that SP (that originally had passed a screen with a mesh aperture of 75 μm) rapidly swell in the water used in the PSD analysis (Fig. 1; Table 1). Statistically, the uniformity parameter (describing the distribution spread) was significantly lower (i.e., narrower) for dispersions without AS (0.6) than for those having AS added (ca. 0.7) (Table 1). The  $D_{4,3}$  diameter (volume-weighted mean) in SP particles and SP dispersions was ca. 80 μm, larger than dispersions containing AS (ca. 70 μm). During the blending process, a slight mechanical disruption of cells of *D. antarctica* could lead to the formation of clusters when SP particles are in dispersions, as was reported by Malafronte et al. (2021) for seaweed suspensions and Ben Tobin et al. (2020) for broccoli suspensions. The addition of AS to SP dispersions decreased the  $D_{4,3}$  diameter on cell clusters, possibly due to the action of salts or ions present in AS.

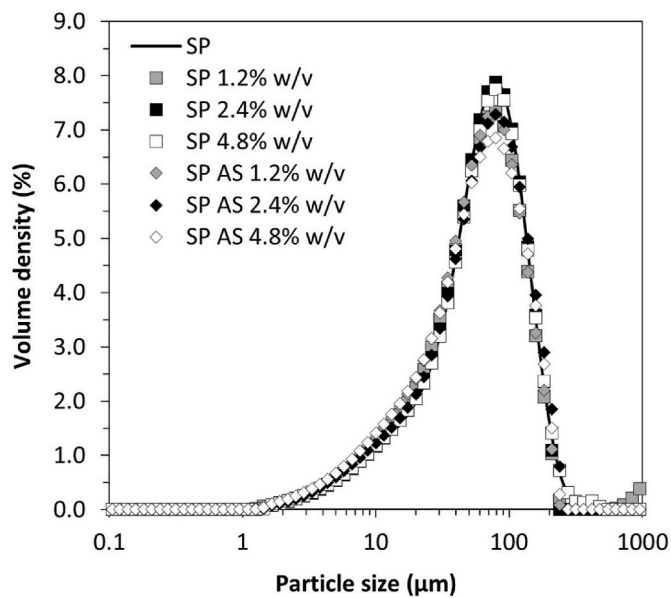


Fig. 1. Particle size distribution of *Durvillaea antarctica* as dry seaweed particles (SP) and SP dispersions in the absence (square symbols) and presence of artificial saliva (AS) (rhombus symbols) measured at room temperature.

### 3.2. Microstructural aspects

Fig. 2 shows photomicrographs obtained by light microscopy of the dry SP and aqueous SP dispersions at different concentrations, providing valuable information regarding changes during hydration. Even though alginates are commercially extracted under aqueous acidic or alkaline conditions (Bojorges, López-Rubio, Martínez-Abad, & Fabra, 2023), polysaccharides also became solubilized when broken cells in *D. antarctica* powder are exposed to water (Saravana, Cho, Woo, & Chun, 2018). Soluble solids varied from 37% to 51% d. w., as the concentration of SP in dispersions changed from 4.8% w/v to 1.2% w/v (Table A1). These values are similar to those reported for seaweed suspensions treated by physical and thermal treatments (Malafrente et al., 2021). Thus, SP dispersions consisted of soft, hydrated seaweed remnants (ghosts) dispersed in a dilute polysaccharide solution (Fig. 2), as also reported by Malafrente et al. (2021). The molecular characterization of the soluble fraction of *D. antarctica* SP dispersions should be further studied.

FESEM images (Fig. 3, left) showed that the original dry SP particles had irregular forms and different sizes. The image of the freeze-dried sample of the SP dispersion at 4.8% w/v (Fig. 3, right) should be analyzed with attention due to artifacts produced during sample preparation. The rather smooth surface corresponds to the deposition of the soluble solids in the suspensions (37%–51% of the total mass of solids) onto particles during freeze-drying and the presence of bulges on the surface (yellow arrows), suggests hidden seaweed particles underneath.

Table 1

Particle size analysis expressed as d (0,9), D [4,3] (µm), and uniformity of *Durvillaea antarctica* as dry SP and in SP aqueous dispersions. Different letters indicate statistical differences ( $p < 0.05$ ).

PSD	Treatment	Seaweed powder <sup>a</sup>		Concentration (% w/v)							
				1.2		2.4		4.8			
d (0,9)	Without AS	150.87	± 0.29 <sup>a</sup>	142.49	± 1.03 <sup>b</sup>	144.99	± 0.59 <sup>c</sup>	152.71	± 1.06 <sup>f</sup>		
	With AS			139.83	± 0.92 <sup>d</sup>	142.25	± 0.74 <sup>e</sup>	150.98	± 1.08 <sup>a</sup>		
D [4,3] (µm)	Without AS	79.44	± 0.59 <sup>a</sup>	72.56	± 0.58 <sup>b</sup>	74.70	± 0.33 <sup>c</sup>	78.96	± 0.55 <sup>a</sup>		
	With AS			71.08	± 1.59 <sup>d</sup>	69.60	± 2.96 <sup>e</sup>	73.05	± 1.39 <sup>f</sup>		
Uniformity	Without AS	0.61	± 0.00 <sup>a</sup>	0.61	± 0.01 <sup>a</sup>	0.59	± 0.00 <sup>b</sup>	0.63	± 0.01 <sup>c</sup>		
	With AS			0.64	± 0.00 <sup>d</sup>	0.70	± 0.01 <sup>e</sup>	0.67	± 0.00 <sup>f</sup>		

<sup>a</sup> Particles were hydrated in the equipment.

Artifacts are common in SEM images of solutions with a high solute content, which leads to distorted morphologies and structural rearranging of molecules (Kaberova et al., 2020).

### 3.3. Viscosity

In rheometry, narrow-gap cone-plate geometry has the advantage that the whole sample is subjected to the same shear rate. The 27 µm gap used in the experiments had the limitation of excluding some large particles in seaweed suspensions. Nevertheless, as appreciated in Figs. 1 and 3 (left), a significant proportion of seaweed particles (e.g., by number) were smaller than the average particle size, so they were included in the experimental sample.

Thickeners for liquids are usually evaluated in the range of shear viscosity between 0.1 and 100 s<sup>-1</sup> and in aqueous dispersions of less than 5% concentration (Hadde et al., 2019; Torres et al., 2019). Fig. 4 shows the flow curves of SP, TU, and TE dispersions at different concentrations in the presence and absence of AS. All samples presented a non-Newtonian shear-thinning behavior, i.e., the apparent shear viscosity decreased as the shear rate increased, which is in agreement with the pseudoplastic behavior of polysaccharides solutions in water and dispersions of soft particles in polysaccharide solutions (Badia-Olmos, Laguna, Rizo, & Tárrega, 2022; Chojnicka-Paszun et al., 2014; Kongjaroen et al., 2022; Vieira et al., 2020).

Apparent shear viscosity increased proportionally with the concentration of SP dispersions and thickeners, either without or with AS (Fig. 4). SP dispersions exhibited a shear-thinning behavior particularly pronounced at concentrations of 2.4% and 4.8% (Fig. 4 b-c). Malafrente et al. (2021) attributed the shear-thinning behavior of seaweed particle dispersions to forming clusters of cell remnants dispersed in a solution of released biopolymers. The supernatant of *D. antarctica* SP dispersions, composed mainly of extracted biopolymers, showed a non-Newtonian behavior, particularly in the range of shear rates between 0.1 and 1.0 s<sup>-1</sup> and after that, the viscosity remained almost constant at 0.01 Pa s (Fig. A1). Thus, the pseudo-plastic behavior of SP suspensions may be explained by the presence of soft ghost particles in a partly non-Newtonian liquid phase (Fig. 3). The increase in apparent viscosity of SP dispersions with higher volumes of the particle fraction in the dispersed phase (e.g., concentration) could be attributed to particle-particle interactions (Herz, Moll, Schmitt, & Weiss, 2023) and probably by the presence of alginate or fucoidans known by their gel-forming capacity (Flórez-Fernández et al., 2019) as demonstrated by Malafrente et al. (2021) for brown macroalgae suspensions, but these issues need further confirmation. Flow curves for TU dispersions (xanthan gum-based) followed the same trend reported by Chojnicka-Paszun et al. (2014) for 2% xanthan gum solution. Flow curves of TE dispersions at 1.2% and 2.4% almost overlapped the SP curves up to a shear rate of 10 s<sup>-1</sup>, while at 4.8%, the initial viscosity was almost one-order magnitude higher (Fig. 4).

The addition of AS resulted in a downshift in most of the flow curves. This could be attributed to the dilution effect (dispersion:saliva ratio is 1:0.5), as well as factors related to the interaction between saliva

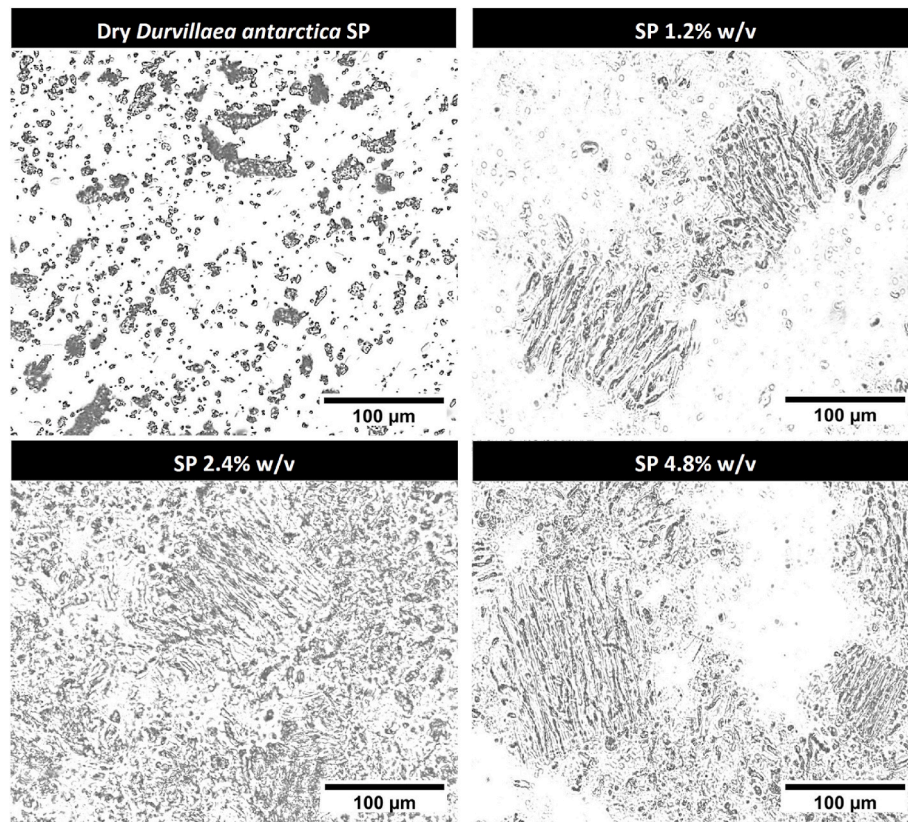


Fig. 2. Light microscopy images of dry SP and SP aqueous dispersions at 1.2% w/v, 2.4% w/v, and 4.8% w/v.

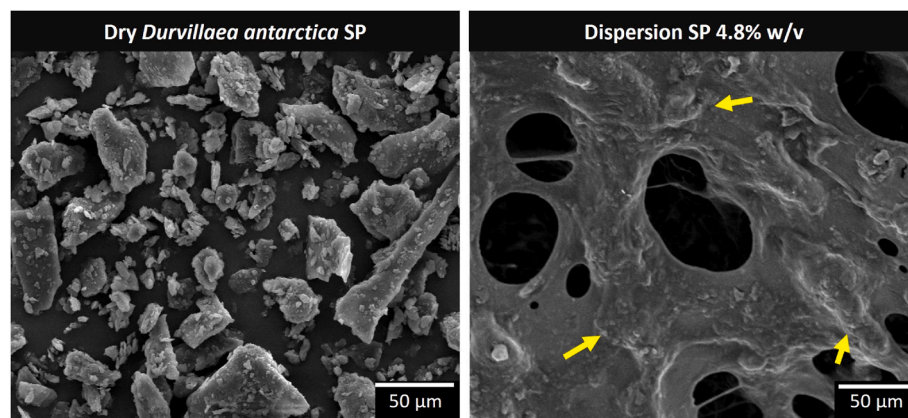
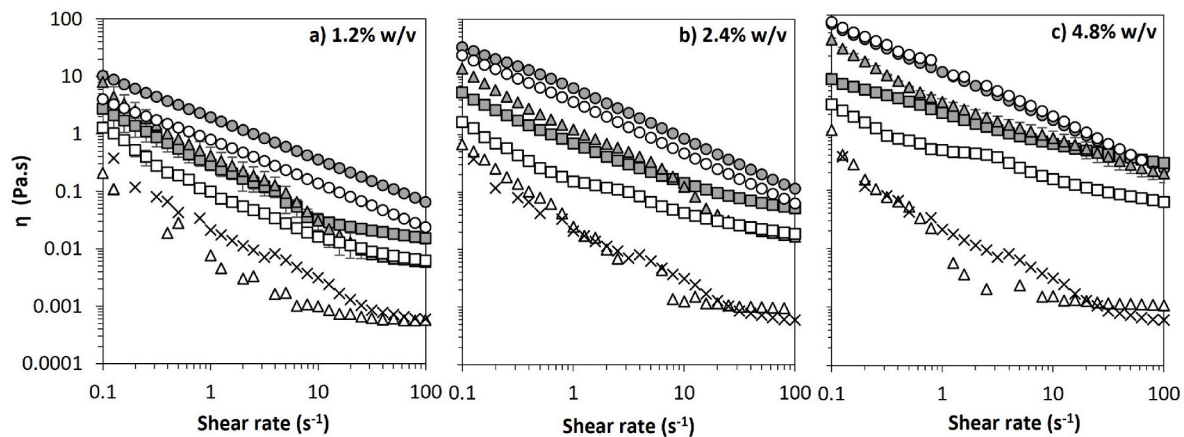


Fig. 3. Scanning electron photomicrographs of seaweed powder SP (left), and a freeze-dried sample of a 4.8% w/v SP dispersion (right). Yellow arrows point to possible remnants of seaweed particles (ghosts) hidden underneath a layer of dry soluble solids.

compounds and thickeners. These results show that a large decrease in the thickening capacity of TE occurred in the whole range of shear rates when AS was added, suggesting a hydrolyzing effect of alpha-amylase owing to the breakdown of starch O-glycosidic bonds (Baixauli et al., 2023; Torres et al., 2019). Hanson, O'Leary, and Smith (2012) also found a fast and pronounced reduction in viscosity when saliva was added to drinks that had been thickened with a mixture containing maize starch. Dispersions of 1.2% SP with AS (Fig. 4a) exhibited a decrease in viscosity of ca. 50%, while the viscosity of TE suspensions with AS decreased almost one order of magnitude. At a concentration of 1.2% in TU thickener, the addition of AS resulted in a dilution effect, as previously reported for a xanthan gum solution at 1% (Torres et al., 2019). Interestingly, in the case of TU, the difference in viscosity between suspensions with and without saliva decreases as the

concentration increases, eventually reaching an overlap when the concentration reaches 4.8% w/v. This suggests an interaction between xanthan gum with components of the artificial saliva, e.g., mucins and ions (Fig. 4c).

Shear-thinning behavior of thickened aqueous dispersions was modeled according to a power-law equation, i.e.,  $\eta(\dot{\gamma}) = K(\dot{\gamma})^{n-1}$ , where  $K$  is the consistency index ( $\text{Pa}\cdot\text{s}^n$ ), and  $n$  the flow behavior index (dimensionless).  $K$  represents the internal structure of the fluid, and a high value of  $K$  means a high consistency. Significant differences ( $p < 0.05$ ) show that  $K$  values increased as the concentration of SP, TU, and TE increased despite the addition of saliva (Table 2). The highest value of  $K$  was for the 4.8% TU dispersion, having added AS ( $11.9 \text{ Pa}\cdot\text{s}^n$ ), while the lowest  $K$  was for the 1.2% TE suspension with AS. All SP dispersions without AS had lower  $K$  values than the corresponding



**Fig. 4.** Shear viscosity as a function of shear rate for SP (□), TU (○), and TE (Δ) dispersions at concentrations of a) 1.2% w/v, b) 2.4% w/v, and c) 4.8% w/v, without AS (solid symbols), with AS (open symbols), and artificial saliva (x).

**Table 2**

Parameters of the Ostwald de Waele model fitted to the shear viscosity data of SP and commercial thickeners TU and TE dispersions with and without artificial saliva (AS) ( $R^2$  0.80–0.99). Different lowercase denotes statistically significant differences ( $p < 0.05$ ).

Dispersions %w/v		Ostwald de Waele fit: $\eta(\dot{\gamma}) = K(\dot{\gamma})^{n-1}$				Relative thixotropic area % <sup>a</sup>			
		K (Pa.s <sup>n</sup> )		n		Without AS		With AS	
		Without AS	With AS	Without AS	With AS	Without AS	With AS	Without AS	With AS
1.2	SP	0.31 ± 0.08 <sup>a</sup>	0.12 ± 0.01 <sup>a</sup>	0.21 ± 0.10 <sup>a</sup>	0.23 ± 0.00 <sup>a</sup>	-9.84 ± 5.54 <sup>a</sup>	1.85 ± 2.35 <sup>b</sup>		
	TU	1.92 ± 0.25 <sup>b</sup>	0.75 ± 0.01 <sup>ab</sup>	0.27 ± 0.00 <sup>a</sup>	0.26 ± 0.01 <sup>a</sup>	12.90 ± 3.55 <sup>c</sup>	2.08 ± 0.61 <sup>b</sup>		
	TE	0.43 ± 0.13 <sup>ab</sup>	0.01 ± 0.01 <sup>a</sup>	0.05 ± 0.04 <sup>abc</sup>	0.27 ± 0.08 <sup>abc</sup>	5.54 ± 23.67 <sup>b</sup>	7.80 ± 0.19 <sup>b</sup>		
2.4	SP	0.78 ± 0.03 <sup>ab</sup>	0.21 ± 0.04 <sup>a</sup>	0.33 ± 0.01 <sup>ad</sup>	0.38 ± 0.05 <sup>ad</sup>	11.58 ± 4.84 <sup>e</sup>	-20.20 ± 8.61 <sup>ad</sup>		
	TU	5.77 ± 0.3 <sup>c</sup>	3.48 ± 0.05 <sup>c</sup>	0.16 ± 0.01 <sup>b</sup>	0.13 ± 0.02 <sup>b</sup>	2.74 ± 0.23 <sup>b</sup>	3.16 ± 4.23 <sup>b</sup>		
	TE	1.22 ± 0.17 <sup>ab</sup>	0.04 ± 0.00 <sup>a</sup>	0.06 ± 0.03 <sup>c</sup>	0.05 ± 0.04 <sup>c</sup>	30.62 ± 13.12 <sup>c</sup>	4.88 ± 5.39 <sup>b</sup>		
4.8	SP	2.19 ± 0.13 <sup>b</sup>	0.58 ± 0.11 <sup>ab</sup>	0.51 ± 0.02 <sup>d</sup>	0.48 ± 0.02 <sup>d</sup>	1.24 ± 1.20 <sup>b</sup>	-10.66 ± 3.29 <sup>a</sup>		
	TU	10.42 ± 0.09 <sup>d</sup>	11.86 ± 1.33 <sup>d</sup>	0.18 ± 0.00 <sup>bc</sup>	0.16 ± 0.01 <sup>b</sup>	5.26 ± 0.63 <sup>b</sup>	3.12 ± 0.76 <sup>b</sup>		
	TE	4.14 ± 0.59 <sup>e</sup>	0.02 ± 0.01 <sup>a</sup>	0.28 ± 0.05 <sup>bc</sup>	0.23 ± 0.17 <sup>bc</sup>	-10.22 ± 0.20 <sup>a</sup>	-53.65 ± 19.47 <sup>d</sup>		

<sup>a</sup> Flow behavior curves of shear stress as a function of shear rate fitted to the power law model (Supplementary Material Fig. A2).

commercial thickeners, suggesting a weaker consistency. In the case of SP dispersions, the K values were not significantly different from those of TE dispersions, except at 4.8% concentration, and a loss of consistency resulted when AS was added (Table 2). For TE dispersions, alpha-amylase in artificial saliva hydrolyzed the starch, decreasing the value of K and confirming the viscosity results shown in Fig. 4 and those presented by Torres et al. (2019) and Baixauli et al. (2023). The n values of SP, TU, and TE dispersions without and with AS varied from 0.05 to 0.51 for the whole range of concentrations (Table 2). TU dispersions exhibited the lowest n values (high shear-thinning effect) at their 2.4% w/v, while SP dispersions, n values increased as the concentration increased, which was attributed to viscous forces of ghost particles in the liquid phase. It is noteworthy that lower n values correspond to TE dispersions where flow curves exhibited a slight Newtonian plateau at a high shear rate (Fig. 4) with a low fitting power law model ( $R^2 \sim 0.80$ ). This flow behavior is not attributed to a higher shear-thinning effect but to an early deformation of TE dispersions that affect the thickening capacity.

Regarding time dependence of dispersions, at 2.4% in the absence of AS, all dispersions resulted in a thixotropic behavior, where SP and TU dispersions exhibited more rheological stability than TE dispersions. TE exhibited an anti-thixotropic behavior at 4.8% in the presence and absence of AS (Table 2). Maize starch dispersions often exhibit an anti-thixotropic behavior under steady shearing ascribed to the rearrangement of the amylopectin molecules (Wang, Li, Wang, & Özkan, 2010). However, Badia-Olmos et al. (2022) proposed that the slow hydration of pre-gelatinized starch thickeners hinders thickening capacity, suggesting that viscosity increases after the flow test. In the case of SP

dispersions, at 2.4% and 4.8% in the presence of AS, there was an anti-thixotropic behavior due to a delay in the rearrangement of SP particles within the continuous phase. TU (gum-based thickener) showed a thixotropic behavior within concentration ranges, attributed to a stable microstructure, i.e., a decreased hysteresis loop (Table 2, Fig. A2) (Fan et al., 2022).

During oral processing and deglutition, food boluses are exposed to different shear rates, namely, around  $10 \text{ s}^{-1}$  and  $50 \text{ s}^{-1}$  in the oral phase and  $100$  or  $300 \text{ s}^{-1}$  in the pharynx (Bolivar-Prados et al., 2021; Nishinari, Turcanu, Nakauma, & Fang, 2019; Ong, Steele, & Duizer, 2018). Fig. 5 shows the apparent viscosity of each sample (with and without added saliva) at shear rates of  $1$ ,  $50$ , and  $100 \text{ s}^{-1}$ . Viscosity at a shear rate of  $50 \text{ s}^{-1}$  is an important criterion in the evaluation of thickeners for dysphagia patients, and it has led to the following classification of fluid foods:  $0.051$ – $0.35 \text{ Pa s}$ , nectar-like;  $0.351$ – $1.750 \text{ Pa s}$ , honey-like,  $>1.750 \text{ Pa s}$ , spoon thick (Cichero et al., 2017). According to the above classification, SP dispersions at a shear rate of  $50 \text{ s}^{-1}$  had a nectar-like consistency (Fig. 5), and the presence of AS (Fig. 5b) could be an approach to the response in swallowing to  $100 \text{ s}^{-1}$ . This suggests that the small hydrated and soft seaweed particles (e.g.,  $<150 \mu\text{m}$ ) could increase the viscosity of aqueous solutions (or thin liquids), and they would probably be only slightly perceived in the mouth, given their low concentrations and the matrix phase viscosity (Chojnicka-Paszun et al., 2014; Shewan, Stokes, & Smyth, 2020), but sensory studies are necessary. Alternatively, particle size reduction of seaweed suspensions may be further achieved by high-pressure homogenization (Malafrente et al., 2021). Thus, *D. antarctica* seaweed powder could find applications in swallowing pathologies, reducing the risk of aspiration (Nishinari et al.,

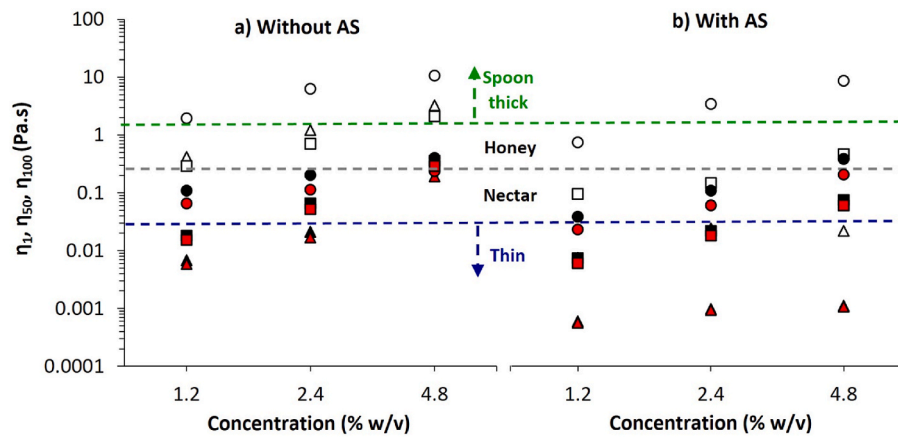


Fig. 5. Apparent viscosity of SP ( $\square$ ), TU (o), TE ( $\Delta$ ) dispersions at shear rates of  $1 \text{ s}^{-1}$  ( $\eta_1$ , open symbols),  $50 \text{ s}^{-1}$  ( $\eta_{50}$ , black symbols), and  $100 \text{ s}^{-1}$  ( $\eta_{100}$ , red symbols) as a function of concentrations at 1.2% w/v, 2.4% w/v, and 4.8% w/v: a) without AS and b) with AS. The dotted lines represent the viscosity ranges of the IDDSI consistency classification at  $50 \text{ s}^{-1}$ .

2019).

### 3.4. Viscoelastic behavior

The viscoelastic characteristics of the SP, TU, and TE dispersions also depended on the concentration and the presence of saliva. Fig. 6 shows the frequency sweeps and resulting storage ( $G'$ ) and loss ( $G''$ ) moduli as a function of angular frequency (rad/s). A solid-like behavior predominates for all dispersions, with and without AS, since  $G'$  remained higher than  $G''$  in the entire frequency sweep, suggesting a weak gel-like behavior ( $G' > G''$ ).  $G'$  and  $G''$  remained almost parallel or changed slightly with frequency in SP and TE dispersions without AS (Fig. 6). These results are in good agreement with previous works on aqueous solutions thickened with modified maize starch at 4.5%–6.0% w/v (Hadde, Chen, & Chen, 2020), polysaccharides extracted from seaweed (Gao et al., 2018) and seaweed suspensions at 5% w/w (Malafronte et al., 2021). At 4.8% w/v concentration and without AS, the TE dispersion exhibited a higher solid-like behavior than SP and TU dispersions, which overlapped starting at a frequency of 4 rad/s ( $G' \sim 27 \text{ Pa}$ ), suggesting a similar viscoelastic behavior (Fig. 6c).

In the absence of artificial saliva, TU dispersions at 2.4% w/v exhibited a pronounced elastic behavior above 2 rad/s compared to SP and TE dispersions (Fig. 6b), which can be attributed to a stable network structure due to the entanglement of the dispersed xanthan gum. Although the addition of AS had a dilution effect of ca. 50% at concentrations of 1.2% w/v and 2.4% w/v, at the concentration of 4.8% w/v, the addition of AS increased  $G'$  ca. 25% with a pronounced solid-like behavior compared to SP and TE dispersions. This suggests that with an increase in the concentration of TU thickener, there may be an interaction between mucins-salts of AS and xanthan gum (Fig. 6c). Similar results have been observed for other xanthan gum thickeners (Funami et al., 2017; Hadde et al., 2019; Kongjaroen et al., 2022).

Dispersions in simulated oral conditions (i.e., adding artificial saliva) exhibited a significant two-order-of-magnitude drop on  $G'$  and  $G''$  values in TE dispersions, which suggests not only a dilution effect but also a loss of structure due to the previously discussed hydrolysis of starch by alpha-amylase. However, SP dispersions with AS at 1.2% w/v showed increased  $G'$  and  $G''$  by ca. 20%. Interestingly, in the case of 2.4% w/v SP, in the presence of artificial saliva,  $G'$  increased by ca. 65%. These results can be attributed to an interaction between the saliva components and SP particles.  $G'$  was higher than  $G''$  for all concentrations of SP, suggesting a weak gel-like behavior perceived in the mouth. Changes in viscoelastic properties of SP dispersions may be due to concentration effects, particle-polymer, and polymer-salts-mucin interactions. The increase in  $G'$  with the concentration of SP dispersions could be

explained by a network-forming capacity of SP particles in the liquid phase and the released polysaccharides (Herz et al., 2023; Malafronte et al., 2021).

### 3.5. Tribological measurements and lubricant effect

Results of the tribological experiments are represented by Stribeck plots of the coefficient of friction (CoF) as a function of the rolling speed (Fig. 7). Each curve is usually divided into three lubrication or friction regimes depending on the increasing thickness of the lubricant film: a boundary regime of high and almost constant frictional resistance (thin film), the mixed regime of decreasing CoF, and the hydrodynamic regime of low frictional resistance (full film). The boundary and mixed regime are dominated by surface properties, while the hydrodynamic lubrication depends on the bulk properties of a thick film (Rudge et al., 2019). The CoF of all studied dispersions followed the behavior of a Stribeck curve with CoF values located below the curve for distilled water that provided a poor lubrication effect (CoF close to 1 up to 100 mm/s) (Fig. 7). Artificial saliva also measured, experienced a large drop from CoF = 0.8 at speeds higher than 4 mm/s, corroborating values reported in previous studies (Bongaerts, Rossetti, & Stokes, 2007; Sarkar et al., 2019). The presence of a short boundary regime and an extended hydrodynamic friction regime, where viscosity dominates, was due to the presence of a thick film separating the PDMS surfaces in the latter case. A large volume of suspension entraining more particles (at 4.8 % w/v) better supported the fluid pressure between the sliding surfaces, resulting in a higher CoF than in 1.2% w/v and 2.4% w/v suspensions (Stokes, Macakova, Chojnicka-Paszun, De Kruif, & De Jongh, 2011).

SP dispersions at all concentrations exhibited the three lubrication regimes (Fig. 7 a-c). In the mixed regime (e.g., between 10 and 100 mm/s), SP dispersions without and with AS at 1.2% and 2.4% concentrations had lower CoF than commercial thickener dispersions (Fig. 7a and b), which could represent a good lubricant by ghost particles released to the liquid phase (Fig. A3). Likely, ghost SP particles could contribute to the lubricant effect (Fig. A3). Also, components such as proteins, fiber, and lipids have been reported to reduce friction and increase lubrication (Fan et al., 2022). In the boundary friction regime, as the concentration of SP and TU dispersions in the absence and presence of AS increased, the CoF and rolling speed decreased (Fig. 7a–c). This suggests that an increase of particles in dispersions is enough to support the load exerted for hydrodynamic forces on the fluid at a low sliding speed range (until  $\sim 5 \text{ mm/s}$ ) (Fig. 7c) (Pradal & Stokes, 2016).

Additionally, the coefficient of friction can be analyzed at high shear rate viscosity measurements since it has been determined that in the contact gap in soft tribology, shear rates of  $1000 \text{ s}^{-1}$  to  $10,000 \text{ s}^{-1}$  are

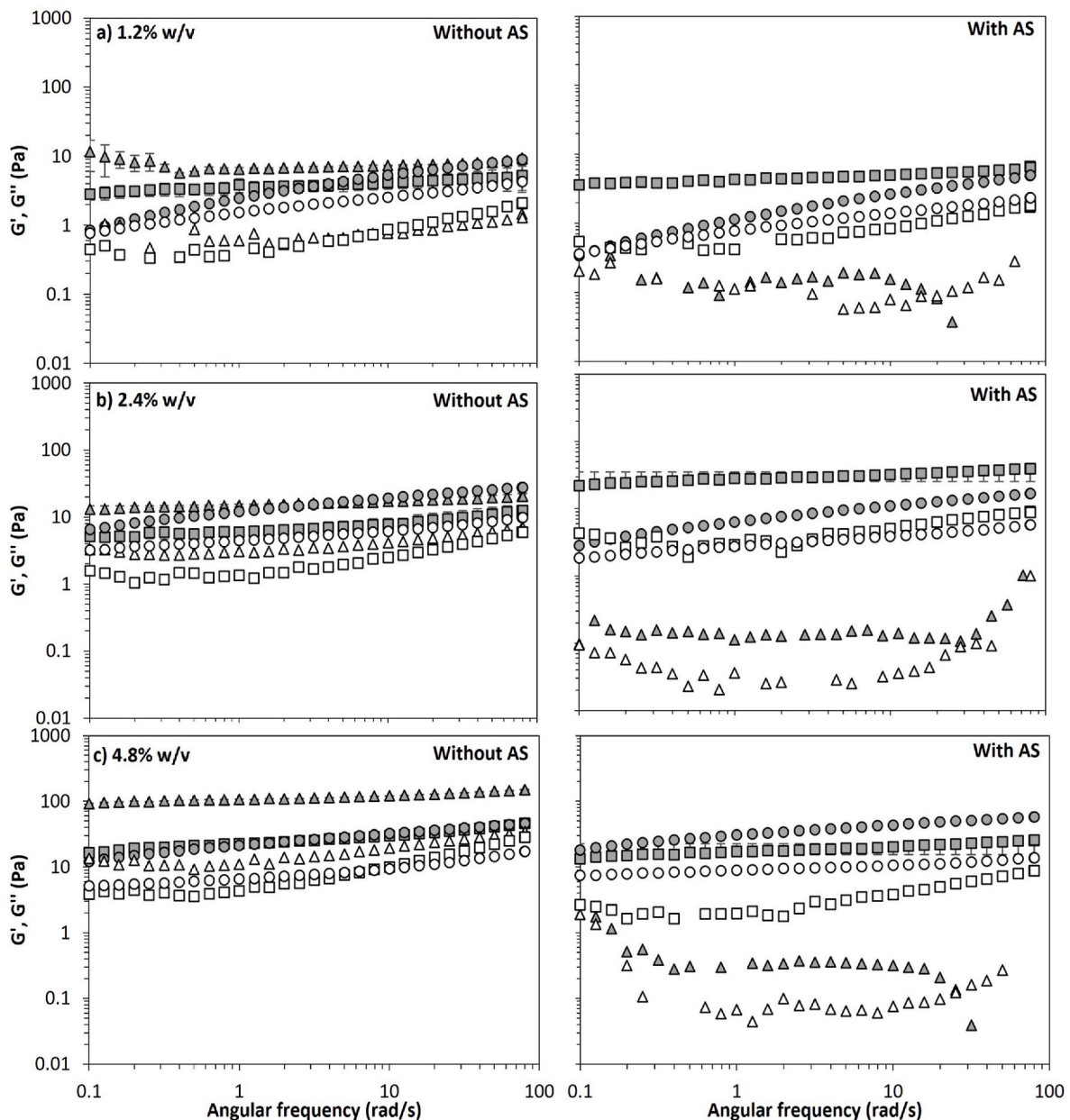


**Fig. 6.** Storage modulus  $G'$  (Pa) (solid symbols) and loss modulus  $G''$  (Pa) (open symbols) from oscillatory frequency sweeps of SP ( $\square$ ), TU ( $\circ$ ), and TE ( $\Delta$ ) dispersions at concentrations of a) 1.2% w/v, b) 2.4% w/v, and c) 4.8% w/v. Without AS (left plot) and with AS (right plot).

present. Interestingly, xanthan gum fluids behave as Newtonian with constant apparent viscosity (De Vicente, Stokes, & Spikes, 2006; Stokes et al., 2011). This analysis is a limitation of our study because our viscosity measurements are up to  $100 \text{ s}^{-1}$ , simulating oral conditions (i.e., using artificial saliva). However, it is relevant to understand the friction mechanism of thickeners used and SP dispersions in oral processing under these conditions. If the data are analyzed by plotting the product of rolling speed times viscosity (at  $100 \text{ s}^{-1}$  in this case) versus the CoF (not shown), as proposed by Bongaerts, Fourtouni, & Stokes (2007); at low concentrations, i.e., 1.2% and 2.4% w/v, it reveals that the boundary regime lubrication of SP suspensions could be mediated by interactions between non-homogeneous “ghost” of SP particles with hydrocolloids, that support the load applied on surfaces allowing the formation of a viscous layer (thinner than particle size), which decreases the CoF (Fig. 7). In contrast, the semi-rigid structure of the xanthan gum of the TU thickener permits film formation that can change slightly with the shear rate, allowing the fluid to entrain between surfaces, thereby

decreasing CoF (De Vicente et al., 2006). In the modified maize starch of the TE thickener, the viscosity is nearly two orders of magnitude lower than that of TU and SP (Fig. 4 a-b). The friction mechanism of the swollen particles TE suggests an adhesion to the surfaces, which increases the CoF until  $\sim 20 \text{ mm/s}$  ( $0.001 U\eta$  not shown), after which the fluid is entrained, decreasing CoF. As concentration increases to 4.8% w/v, the curves of the thickener dispersions, including SP, shift to hydrodynamic zones, indicating that the friction mechanism is mediated by viscosity. Accordingly, soft particles and viscosity are responsible for the lubrication in the mixed regime in SP dispersions, while bulk properties dominate in TU and TE.

Notably, in the boundary and mixed regime at 1.2% and 2.4% w/v, in the transitional point between the mixed and hydrodynamic regime (about  $100 \text{ mm/s}$ ), the coefficient of friction was lower in SP dispersions ( $\text{CoF} \sim 0.002$ ) than in commercial thickeners ( $\text{CoF} \sim 0.005$ ). TE thickener failed in low concentrations and showed a poor lubricant effect compared to SP and TU samples (Fig. 7 a-b). On the other hand, the

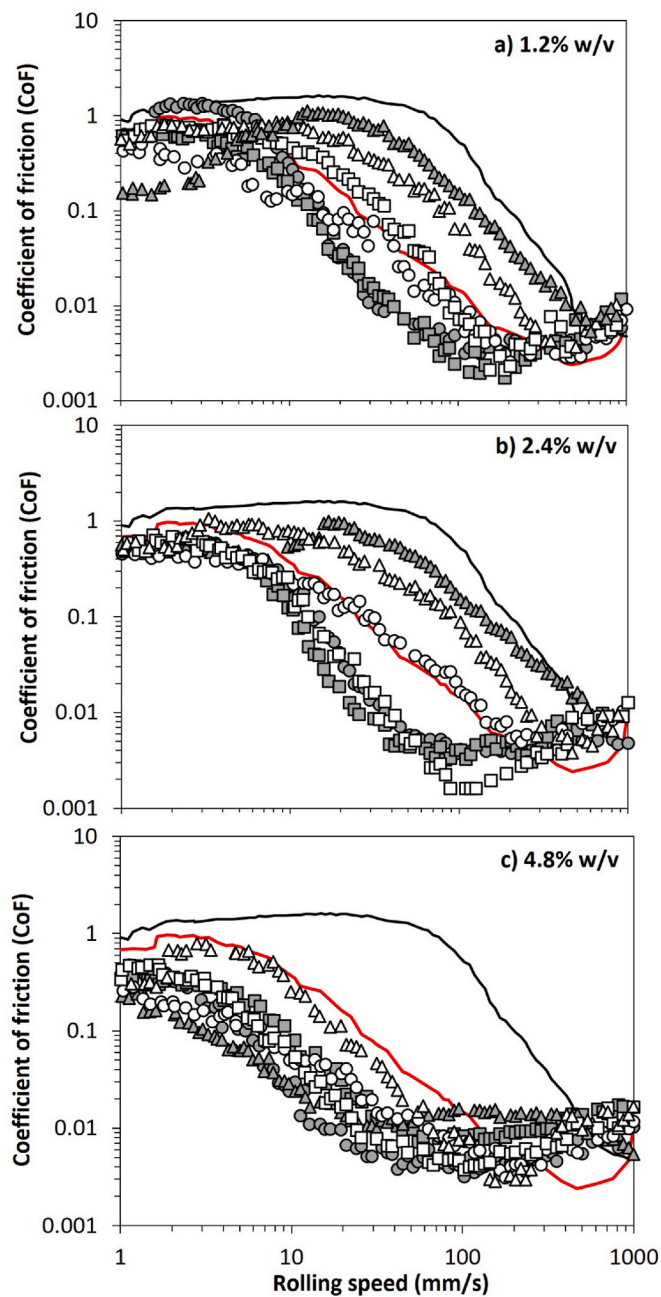


**Fig. 7.** Stribeck curves of SP ( $\square$ ), TU ( $\circ$ ), and TE ( $\Delta$ ) dispersions at concentrations of a) 1.2% w/v, b) 2.4% w/v, and c) 4.8% w/v. Without AS (solid symbols) and with AS (open symbols). Solid lines represent the behavior of artificial saliva (red) and distilled water (black).

addition of AS seems not to affect the CoF in SP dispersions, while in the case of TU samples the overlapping of the AS curve in 1.2% and 2.4% w/v suggests a possible interaction between saliva components and TU that decrease CoF, as was proposed by Torres et al. (2019). For the 4.8% w/v concentration, all samples exhibited better lubricating properties than saliva. Nevertheless, it is important to note that the correction of high shear rate viscosity could corroborate this analysis.

It has been reported that xanthan gum in low concentrations does not exhibit boundary lubrication, and its CoF is similar to that of water, which is corroborated in Fig. 7a for the TU thickener (De Vicente, Stokes, & Spikes, 2005). The lubricant effect of the TU thickener was dependent on concentration, similar to findings for xanthan gum solutions between 1% and 4% (Chojnicka-Paszun et al., 2014). The addition

of artificial saliva caused a decrease in CoF by about 60%, and a similar behavior was observed for a xanthan gum-based thickener (1%) in the presence of artificial saliva (Baixauli et al., 2023; Torres et al., 2019). The TE thickener resulted in a clear lubricant effect at a concentration of 4.8% dispersions at low rolling speeds ( $\sim 2$  mm/s), and lubrication was dominated by bulk properties since there was a drop of TE towards the mixed regime (Fig. 7c). Similar results were reported for native maize starch suspensions (Zhang et al., 2017). However, in the presence of AS, the hydrolyzing effect of alpha-amylase made the lubricant effect mostly due to the mucin of artificial saliva overlapping the artificial saliva curve (Fig. 7c) (Torres et al., 2019).

Results from the Stribeck curves in Fig. 7 could be further analyzed considering the speeds experienced during oral processing and swallowing. In the case of liquid foods, the tongue moves through the oral cavity at speeds from around 10 to 300 mm/s (Hiemae & Palmer, 2003). The velocity spectrum of bolus flow in the pharynx (that is viscosity-dependent) has an average of around 100 mm/s and shows a maximum velocity of 500 mm/s for water and 200 mm/s for yogurt (Chen, 2009). Moreover, in the human whole saliva, the CoF values smaller than 0.1 in smooth PDMS tribopairs may be considered an efficient lubricant compared to water of CoF ca. 1 (Bongaerts et al., 2007). Under these conditions, both in the boundary and mixed regime, all SP suspensions in this study provide a lubrication effect.

#### 4. Conclusions

Food thickeners are used to modify the textural perception of liquid foods in a variety of applications. Seaweeds are cheap, abundant, and sustainable sources of food as well as carriers of polysaccharides and bioactive compounds that deserve their study in novel applications. Commercial thickeners based on refined hydrocolloids play important roles in modifying the viscosity, viscoelastic, and lubrication properties of liquid foods during oral processing and swallowing. Aqueous suspensions of fine particles of the seaweed *D. antarctica* (SP) exhibited behavior in these three dimensions comparable to those of two commercially formulated thickeners and in an ample range of operational values that would permit satisfying several applications. The addition of artificial saliva, which better simulates conditions in the oral cavity, proved to modify the tribo-rheological behavior of samples, often in a drastic form, as was the case of thickeners containing modified starch. We hypothesize that the rheological and lubricant effects of SP particles in an aqueous suspension are due to the released hydrocolloid molecules (as evidenced by the soluble solids content) and the interactions with ghosts of the cellular structure of the seaweed particles. The knowledge of the lubricant, viscosity, and viscoelasticity effects of suspensions of soft seaweed particles in a liquid bolus provides the guidelines to rationally design liquid foods that are sensorially acceptable and physiologically advantageous. Moreover, SP may become a low-cost and sustainable alternative as food thickeners in some applications. Further research should take into consideration the intrinsic variability of the seaweed and aim at determining the molecular composition of the soluble solids fraction, understanding the mechanisms underlying the relation between the rheo-tribological properties of fine SP suspensions with their microstructure, and assessing perceived sensorial properties of SP suspensions (e.g., taste).

#### CRedit authorship contribution statement

**Leyla Covacevich:** Writing – review & editing, Writing – original draft, Visualization, Validation, Methodology, Investigation, Funding acquisition, Formal analysis, Data curation, Conceptualization. **José Miguel Aguilera:** Writing – review & editing, Visualization, Validation, Supervision, Funding acquisition. **M. Carolina Moreno:** Writing – review & editing, Validation, Supervision. **Natalia Brossard:** Validation, Resources, Methodology. **Fernando Osorio:** Resources, Methodology.

## Declaration of competing interest

The authors declare that they have no known competing financial interests or personal relationships that could have appeared to influence the work reported in this paper.

## Data availability

Data will be made available on request.

## Acknowledgements

This work was financially supported by ANID through the Advanced National Human Capital Formation Program – Doctoral Fellowship 2021 (N° 21211089) to author Covacevich. Other funding sources were grants from Fondecyt (Project 1180082) and the Technological Centers of Excellence with Basal Financing, ANID-Chile, to the Cape Horn International Center (CHIC-ANID PIA/BASAL PFB210018).

## Appendix A. Supplementary data

Supplementary data to this article can be found online at <https://doi.org/10.1016/j.foodhyd.2024.110116>.

## References

- Aguilera, J. M., & Covacevich, L. (2023). Designing foods for an increasingly elderly population: A challenge of the XXI century. *Current Opinion in Food Science*, 51, Article 101037. <https://doi.org/10.1016/j.cofs.2023.101037>
- Badia-Olmos, C., Laguna, L., Rizo, A., & Tárrega, A. (2022). Dysphagia thickeners in context of use: Changes in thickened drinks viscosity and thixotropy with temperature and time of consumption. *Journal of Texture Studies*, 53(3), 383–395. <https://doi.org/10.1111/jtxs.12685>
- Baixaui, R., Dobiášová, A., Tárrega, A., & Laguna, L. (2023). Pairing physical and sensory properties of dysphagia thickeners to understand disliking. *Food Hydrocolloids for Health*, 3, Article 100140. <https://doi.org/10.1016/j.fhfh.2023.100140>
- Ben Tobin, A., Mihnea, M., Hildenbrand, M., Miljkovic, A., Garrido-Bañuelos, G., Xanthakis, E., et al. (2020). Bolus rheology and ease of swallowing of particulated semi-solid foods as evaluated by an elderly panel. *Food & Function*, 11(10), 8648–8658. <https://doi.org/10.1039/d0fo01728k>
- Blok, A. E., Bolhuis, D. P., Kibbelaar, H. V. M., Bonn, D., Velikov, K. P., & Stieger, M. (2021). Comparing rheological, tribological, and sensory properties of microfibrillated cellulose dispersions and xanthan gum solutions. *Food Hydrocolloids*, 121, Article 107052. <https://doi.org/10.1016/j.foodhyd.2021.107052>
- Blok, A. E., Bolhuis, D. P., & Stieger, M. (2020). Contributions of viscosity and friction properties to oral and haptic texture perception of iced coffees. *Food & Function*, 11(7), 6446–6457. <https://doi.org/10.1039/D0FO01109F>
- Bojorges, H., López-Rubio, A., Martínez-Abad, A., & Fabra, M. J. (2023). Overview of alginate extraction processes: Impact on alginate molecular structure and techno-functional properties. *Trends in Food Science & Technology*, 140, Article 104142. <https://doi.org/10.1016/j.tifs.2023.104142>
- Bolivar-Prados, M., Tomsen, N., Arenas, C., Ibáñez, L., & Clave, P. (2021). A bit thick: Hidden risks in thickening products' labeling for dysphagia treatment. *Food Hydrocolloids*, 106960. <https://doi.org/10.1016/j.foodhyd.2021.106960>
- Bongaerts, J. H. H., Fournouni, V., & Stokes, J. R. (2007b). Soft-tribology: Lubrication in a compliant PDMS–PDMS contact. *Tribology International*, 40, 1531–1542. <https://doi.org/10.1016/j.triboint.2007.01.007>
- Bongaerts, J. H. H., Rossetti, D., & Stokes, J. R. (2007a). The lubricating properties of human whole saliva. *Tribology Letters*, 27, 277–287. <https://doi.org/10.1007/s11249-007-9232-y>
- Chen, J. (2009). Food oral processing - a review. *Food Hydrocolloids*, 23(1), 1–25. <https://doi.org/10.1016/j.foodhyd.2007.11.013>
- Chojnicka-Paszun, A., Doussinault, S., & De Jongh, H. H. J. (2014). Sensorial analysis of polysaccharide-gelled protein particle dispersions about lubrication and viscosity properties. *Food Research International*, 56, 199–210. <https://doi.org/10.1016/j.foodres.2013.12.035>
- Cichero, J. (2018). Age-related changes to eating and swallowing impact frailty: Aspiration, choking risk, modified food texture, and autonomy of choice. *Geriatrics*, 3(4), 69. <https://doi.org/10.3390/geriatrics3040069>
- Cichero, J. A. Y., Lam, P., Steele, C. M., Hanson, B., Chen, J., Dantas, R. O., et al. (2017). Development of international terminology and definitions for texture-modified foods and thickened fluids used in dysphagia management: The IDDSI framework. *Dysphagia*, 32(2), 293–314. <https://doi.org/10.1007/s00455-016-9758-y>
- De Vicente, J., Stokes, J. R., & Spikes, H. A. (2005). The frictional properties of Newtonian fluids in rolling-sliding soft-EHL contact. *Tribology Letters*, 20, 3–4. <https://doi.org/10.1007/s11249-005-9067-3>
- De Vicente, J., Stokes, J. R., & Spikes, H. A. (2006). Soft lubrication of model hydrocolloids. *Food Hydrocolloids*, 20, 483–491. <https://doi.org/10.1016/j.foodhyd.2005.04.005>
- Devezeaux de Lavergne, M., Van de Velde, F., & Stieger, M. (2017). Bolus matters the influence of food oral breakdown on dynamic texture perception. *Food & Function*, 8(2), 464–480. <https://doi.org/10.1039/c6fo01005a>
- Fan, Y., Zhang, L., Wang, X., Wang, K., Wang, L., Wang, Z., et al. (2022). Rheological thixotropy and pasting properties of food thickening gums orienting at improving food holding rate. *Applied Rheology*, 32(1), 100–121. <https://doi.org/10.1515/arih-2022-0127>
- Figueroa, V., Farfán, M., & Aguilera, J. M. (2021). Seaweeds as novel foods and source of culinary flavors. *Food Reviews International*, 1–24. <https://doi.org/10.1080/87559129.2021.1892749>
- Flórez-Fernández, N., Domínguez, H., & Torres, M. D. (2019). A green approach for alginate extraction from *Sargassum muticum* brown seaweed using ultrasound-assisted technique. *International Journal of Biological Macromolecules*, 124, 451–459. <https://doi.org/10.1016/j.ijbiomac.2018.11.232>
- Funami, T., Matsuyama, S., Ikegami, A., Nakauma, M., Hori, K., & Ono, T. (2017). *In vivo* measurement of swallowing by monitoring thyroid cartilage movement in healthy subjects using thickened liquid samples and its comparison with sensory evaluation. *Journal of Texture Studies*, 48(6), 494–506. <https://doi.org/10.1111/jtxs.12261>
- Gao, H., Duan, B., Lu, A., Deng, H., Du, Y., Shi, X., et al. (2018). Fabrication of cellulose nanofibers from waste brown algae and their potential application as milk thickeners. *Food Hydrocolloids*, 79, 473–481. <https://doi.org/10.1016/j.foodhyd.2018.01.023>
- Gonzalez-Estano, K., Libardi, M., Biasoli, F., & Stieger, M. (2022). Oral processing behaviours of liquid, solid and composite foods are primarily driven by texture, mechanical and lubrication properties rather than by taste intensity. *Food & Function*, 13(9), 5011–5022. <https://doi.org/10.1039/D2FO00300G>
- Hadde, E. K., Chen, W., & Chen, J. (2020). Cohesiveness visual evaluation of thickened fluids. *Food Hydrocolloids*, 101, Article 105522. <https://doi.org/10.1016/j.foodhyd.2019.105522>
- Hadde, E. K., Cichero, J. A. Y., Zhao, S., Chen, W., & Chen, J. (2019). The Importance of extensional rheology in bolus control during swallowing. *Scientific Reports*, 9(1), Article 16106. <https://doi.org/10.1038/s41598-019-52269-4>
- Hanson, B., O'Leary, M. T., & Smith, C. H. (2012). The effect of saliva on the viscosity of thickened drinks. *Dysphagia*, 27(1), 10–19. <https://doi.org/10.1007/s00455-011-9330-8>
- Herz, E., Moll, P., Schmitt, C., & Weiss, J. (2023). Binders in foods: Definition, functionality, and characterization. *Food Hydrocolloids*, 145, Article 109077. <https://doi.org/10.1016/j.foodhyd.2023.109077>
- Hiiemae, K. M., & Palmer, J. B. (2003). Tongue movements in feeding and speech. *Critical Reviews in Oral Biology & Medicine*, 14, 413–429. <https://doi.org/10.1177/154411130301400604>
- Himashree, P., Sengar, A. S., & Sunil, C. K. (2022). Food thickening agents: Sources, chemistry, properties and applications - a review. *International Journal of Gastronomy and Food Science*, 27, Article 100468. <https://doi.org/10.1016/j.ijgfs.2022.100468>
- Jönsson, M., Allahgholi, L., Sardari, R. R., Hreggviðsson, G. O., & Nordberg Karlsson, E. (2020). Extraction and modification of macroalgal polysaccharides for current and next-generation applications. *Molecules*, 25(4), 930. <https://doi.org/10.3390/molecules25040930>
- Kaberova, Z., Karpushkin, E., Nevalová, M., Vetrík, M., Šlouf, M., & Dušková-Smrčková, M. (2020). Microscopic structure of swollen hydrogels by scanning electron and light microscopies: Artifacts and reality. *Polymers*, 12, 578. <https://doi.org/10.3390/polym12030578>
- Kelly, B. J., & Brown, M. T. (2000). Variations in the alginate content and composition of *Durvillaea antarctica* and *D. willana* from southern New Zealand. *Journal of Applied Phycology*, 12, 317–324. <https://doi.org/10.1023/A:1008106723185>
- Kokini, J. L., Kadane, J. B., & Cussler, E. L. (1977). Liquid texture perceived in the mouth. *Journal of Texture Studies*, 8(2), 195–218. <https://doi.org/10.1111/j.1745-4603.1977.tb01175.x>
- Kongjaroen, A., Methacanon, P., & Gamonpilas, C. (2022). On the assessment of shear and extensional rheology of thickened liquids from commercial gum-based thickeners used in dysphagia management. *Journal of Food Engineering*, 316, Article 110820. <https://doi.org/10.1016/j.jfoodeng.2021.110820>
- Krop, E. M., Hetherington, M. M., Holmes, M., Miquel, S., & Sarkar, A. (2019). On relating rheology and oral tribology to sensory properties in hydrogels. *Food Hydrocolloids*, 88, 101–113. <https://doi.org/10.1016/j.foodhyd.2018.09.040>
- Laguna, L., Hetherington, M. M., Chen, J., Artigas, G., & Sarkar, A. (2016). Measuring eating capability, liking and difficulty perception of older adults: A textural consideration. *Food Quality and Preference*, 53, 47–56. <https://doi.org/10.1016/j.foodqual.2016.05.013>
- Malafronte, L., Yilmaz-Turan, S., Krona, A., Martínez-Sanz, M., Vilaplana, F., & Lopez-Sanchez, P. (2021). Macroalgae suspensions prepared by physical treatments: Effect of polysaccharide composition and microstructure on the rheological properties. *Food Hydrocolloids*, 120, Article 106989. <https://doi.org/10.1016/j.foodhyd.2021.106989>
- Mateluna, C., Figueroa, V., Ortiz, J., & Aguilera, J. M. (2020). Effect of processing on texture and microstructure of the seaweed *Durvillaea antarctica*. *Journal of Applied Phycology*, 32(6), 4211–4219. <https://doi.org/10.1007/s10811-020-02259-1>
- Minikus, M., Alminger, M., Alvito, P., Ballance, S., Bohn, T., Bourlieu, C., et al. (2014). A standardised static *in vitro* digestion method suitable for food - an international consensus. *Food & Function*, 5, 1113–1124. <https://doi.org/10.1039/c3fo60702j>
- Nishinari, K., Turcanu, M., Nakauma, M., & Fang, Y. (2019). Role of fluid cohesiveness in safe swallowing. *Npj Science of Food*, 3(1), 1–13. <https://doi.org/10.1038/s41538-019-0038-8>

- Ong, J., Steele, C. M., & Duizer, L. M. (2018). Challenges to assumptions regarding oral shear rate during oral processing and swallowing based on sensory testing with thickened liquids. *Food Hydrocolloids*, *84*, 173–180. <https://doi.org/10.1016/j.foodhyd.2018.05.043>
- Ortiz, J., Romero, N., Robert, P., Araya, J., Lopez-Hernández, J., Bozzo, C., et al. (2006). Dietary fiber, amino acid, fatty acid and tocopherol contents of the edible seaweeds *Ulva lactuca* and *Durvillaea antarctica*. *Food Chemistry*, *99*(1), 98–104. <https://doi.org/10.1016/j.foodchem.2005.07.027>
- Paraskevi, S., Scrinis, G., Huybrechts, I., Woods, J., Vineis, P., & Millett, C. (2020). The neglected environmental impacts of ultra-processed foods. *The Lancet Planetary Health*, *4*(10), e437–e438. [https://doi.org/10.1016/S2542-5196\(20\)30177-7](https://doi.org/10.1016/S2542-5196(20)30177-7)
- Peñalver, R., Lorenzo, J. M., Ros, G., Amarowicz, R., Pateiro, M., & Nieto, G. (2020). Seaweeds as a functional ingredient for a healthy diet. *Marine Drugs*, *18*(6), 301. <https://doi.org/10.3390/md18060301>
- Pradal, C., & Stokes, J. R. (2016). Oral tribology: Bridging the gap between physical measurements and sensory experience. *Current Opinion in Food Science*, *9*, 34–41. <https://doi.org/10.1016/j.cofs.2016.04.008>
- Rioux, L.-E., Beaulieu, L., & Turgeon, S. L. (2017). Seaweeds: A traditional ingredients for new gastronomic sensation. *Food Hydrocolloids*, *68*, 255–265. <https://doi.org/10.1016/j.foodhyd.2017.02.005>
- Rudge, R. E., Scholten, E., & Dijkman, J. A. (2019). Advances and challenges in soft tribology with applications to foods. *Current Opinion in Food Science*, *27*, 90–97. <https://doi.org/10.1016/j.cofs.2019.06.011>
- Saravana, P. S., Cho, Y.-N., Woo, H.-C., & Chun, B.-S. (2018). Green and efficient extraction of polysaccharides from brown seaweed by adding deep eutectic solvent in subcritical water hydrolysis. *Journal of Cleaner Production*, *198*, 1474–1484. <https://doi.org/10.1016/j.jclepro.2018.07.15>
- Sarkar, A., Andablo-Reyes, E., Bryant, M., Dowson, D., & Neville, A. (2019). Lubrication of soft oral surfaces. *Current Opinion in Colloid & Interface Science*, *39*, 61–75. <https://doi.org/10.1016/j.cocis.2019.01.008>
- Schmidt, H., Komoroski, M. R., Steemburgo, T., & Oliveira, V. R. (2021). Influence of thickening agents on rheological properties and sensory attributes of dysphagic diet. *Journal of Texture Studies*, *52*(5–6), 587–602. <https://doi.org/10.1111/jtxs.12596>
- Shewan, H. M., Pradal, C., & Stokes, J. R. (2020). Tribology and its growing use toward the study of food oral processing and sensory perception. *Journal of Texture Studies*, *51*(1), 7–22. <https://doi.org/10.1111/jtxs.12452>
- Shewan, H. M., Stokes, J. R., & Smyth, H. E. (2020). Influence of particle modulus (softness) and matrix rheology on the sensory experience of 'grittiness' and 'smoothness'. *Food Hydrocolloids*, *103*, Article 105662. <https://doi.org/10.1016/j.foodhyd.2020.105662>
- Stokes, J. R., Boehm, M. W., & Baier, S. K. (2013). Oral processing, texture and mouthfeel: From rheology to tribology and beyond. *Current Opinion in Colloid & Interface Science*, *18*(4), 349–359. <https://doi.org/10.1016/j.cocis.2013.04.010>
- Stokes, J. R., Macakova, L., Chojnicka-Paszun, A., De Kruif, C. G., & De Jongh, H. H. J. (2011). Lubrication, adsorption, and rheology of aqueous polysaccharide solutions. *Langmuir*, *27*, 3474–3484. <https://doi.org/10.1021/la104040d>
- Torres, O., Yamada, A., Rigby, N. M., Hanawa, T., Kawano, Y., & Sarkar, A. (2019). Gellan gum: A new member in the dysphagia thickener family. *Biotribology*, *17*, 8–18. <https://doi.org/10.1016/j.biotri.2019.02.002>
- Vieira, J. M., Oliveira, F. D., Salvaro, D. B., Maffezzoli, G. P., de Mello, J. D. B., Vicente, A. A., et al. (2020). Rheology and soft tribology of thickened dispersions aiming the development of oropharyngeal dysphagia-oriented products. *Current Research in Food Science*, *3*, 19–29. <https://doi.org/10.1016/j.crf.2020.02.001>
- Wang, B., Li, D., Wang, L.-J., & Özkan, N. (2010). Anti-thixotropic properties of waxy maize starch dispersions with different pasting conditions. *Carbohydrate Polymers*, *79*(4), 1130–1139. <https://doi.org/10.1016/j.carbpol.2009.10.053>
- Windhab, E. J. (1995). Rheology in food processing. In S. T. Beckett (Ed.), *Physico-chemical aspects of food processing* (pp. 80–116). Springer US. [https://doi.org/10.1007/978-1-4613-1227-7\\_5](https://doi.org/10.1007/978-1-4613-1227-7_5)
- You, K. M., & Sarkar, A. (2021). Oral tribology of polysaccharides. In G. O. Phillips, & P. A. Williams (Eds.), *Handbook of hydrocolloids* (3rd ed., pp. 93–124). Woodhead Publishing. <https://doi.org/10.1016/B978-0-12-820104-6.00008-5>
- Zhang, B., Selway, N., Shelat, K. J., Dhital, S., Stokes, J. R., & Gidley, M. J. (2017). Tribology of swollen starch granule suspensions from maize and potato. *Carbohydrate Polymers*, *155*, 128–135. <https://doi.org/10.1016/j.carbpol.2016.08.064>